A novel DCL2-dependent miRNA pathway in tomato affects susceptibility to RNA viruses

Zhengming Wang,[1] Thomas J. Hardcastle,[1] Alex Canto Pastor,[1] Wing Hin Yip,[2] Shuoya Tang,[1] and David C. Baulcombe[1]

[1]Department of Plant Sciences, University of Cambridge, Cambridge, CB2 3EA, United Kingdom; [2]Department of Biomedical Sciences, City University of Hong Kong, Hong Kong

Tomato Dicer-like2 (slDCL2) is a key component of resistance pathways against potato virus X (PVX) and tobacco mosaic virus (TMV). It is also required for production of endogenous small RNAs, including miR6026 and other noncanonical microRNAs (miRNAs). The *slDCL*2 mRNAs are targets of these slDCL2-dependent RNAs in a feedback loop that was disrupted by target mimic RNAs of miR6026. In lines expressing these RNAs, there was correspondingly enhanced resistance against PVX and TMV. These findings illustrate a novel miRNA pathway in plants and a crop protection strategy in which miRNA target mimicry elevates expression of defense-related mRNAs.

Supplemental material is available for this article.

Received February 26, 2018; revised version accepted June 27, 2018.

RNA silencing plays important roles in plant development, genome stability, and antiviral resistance (Baulcombe 2004). There are multiple pathways of RNA silencing in plants in which small RNAs (sRNAs), ranging from 20 to 24 nucleotides (nt), bind to Argonaute (AGO) effector proteins. The AGO ribonucleoprotein then anneals to a target RNA through Watson–Crick base pairing with an outcome that depends on the nature of the target RNA. If the target RNA is cytoplasmic, there is post-transcriptional gene silencing (PTGS) through cleavage of target RNA and/or translation inhibition (Rogers and Chen 2013), whereas, with nuclear RNA, there may be epigenetic effects in which AGOs recruit DNA/chromatin-modifying factors (Law and Jacobsen 2011).

In plants, the cytoplasmic pathways of RNA silencing involve two different types of sRNA: siRNAs and microRNAs (miRNA). The siRNAs are produced from various types of dsRNA, whereas miRNAs have a hairpin-like RNA precursor in which there are mismatches in the regions of base pairing. In both instances, the processing enzyme is referred to as Dicer-like (DCL).

The siRNA and miRNA pathways interconnect through a complex mechanism involving secondary siRNA production (Allen et al. 2005; Li et al. 2011; Zhai et al. 2011). In the "two-hit" model, a transcript with dual miRNA target sites is the secondary siRNA precursor (Allen et al. 2005), whereas, in the "one-hit" model, the miRNA is typically 22 nt rather than the canonical 21 nt (Chen et al. 2010; Cuperus et al. 2010). In both models, the miRNAs may mediate cleavage of their target RNA, as in the normal miRNA pathway, but there are several additional steps. First, the 3′ cleavage product of the target RNA is converted into a double-stranded form by an RNA-dependent RNA polymerase 6 (RDR6) RNA. The dsRNA is then processed by DCL4 to secondary siRNAs (Allen et al. 2005; Gasciolli et al. 2005).

A distinct feature of these secondary RNAs is that they align predominantly to their template RNA in a phased register in which the first position is opposite position 10 of the initiator miRNA. In some instances, the phasing register has a 21-nt spacing (Allen et al. 2005; Zhai et al. 2011; Creasey et al. 2014), but, in male reproductive organs of monocots, there are also phased secondary sRNAs with a 24-nt register (Johnson et al. 2009).

There are two mechanisms for 22-nt sRNA production. One mechanism, for miRNAs, is based on DCL1 that typically produces 21-nt sRNAs but generates 22-nt products if the precursor RNA has an asymmetric bulge in the base-paired region. Presumably, the bulge allows 22-nt RNA to be accommodated between the DCL active sites on either side of the mature miRNA. The second mechanism of 22-nt sRNA production involves DCL2 and is independent of bulges in the precursor RNA. DCL2 in *Arabidopsis* can process endogenous and viral dsRNA into 22-nt sRNAs when other DCLs, especially DCL4, are absent (Xie et al. 2004; Gasciolli et al. 2005; Bouché et al. 2006). More importantly, DCL2 plays a primary role in transgene silencing, especially in sense transgene-induced silencing and transitivity of hairpin-induced transgene silencing (Mlotshwa et al. 2008; Parent et al. 2015). There is also a role of DCL2 in systematic spreading of transitive silencing between cells and through the vascular system (Taochy et al. 2017; Wu et al. 2017).

In addition to involvement in transgene and viral RNA silencing, there could be secondary sRNA cascades affecting endogenous gene expression and antivirus defense that are also dependent on DCL2 and endogenous 22-nt sRNAs. To investigate this possibility, we analyzed DCL2 isoforms in tomato and found that *slDCL*2a and *slDCL*2b are the most abundantly expressed genes in the four-member *slDCL*2 family. From *sldcl*2ab mutants, we conclude that DCL2 is the major Dicer in tomato defense against tobacco mosaic virus (TMV) and potato virus X (PVX) and that it is involved in the biogenesis of endogenous 22-nt sRNA. The 24-nt sRNA pathways are also influenced by DCL2, both positively and negatively. Among the endogenous 22-nt sRNAs are miRNAs, including miR6026 that targets *slDCL2* mRNA and triggers secondary sRNA production. We disrupted this regulatory feedback loop with target mimic RNAs of miR6026 so that

[*Keywords*: RNA silencing; tomato; Dicer; miRNA; virus]
Corresponding author: dcb40@cam.ac.uk
Article published online ahead of print. Article and publication date are online at http://www.genesdev.org/cgi/doi/10.1101/gad.313601.118.

slDCL2 was up-regulated and antivirus resistance was enhanced. We propose that disruption of this and other defense-related miRNAs could be used as part of an integrated pest management strategy to protect crops against viruses and other pathogens.

Results and Discussion

CRISPR mutants of slDCL2

The tomato genome encodes four isoforms of *slDCL2* (Bai et al. 2012), of which two (*slDCL2a* and *slDCL2b*) are highly expressed in young leaves and two (*slDCL2c* and *slDCL2d*) are barely detectable by RT–PCR (Supplemental Fig. S1). To investigate the functions of *slDCL2*, we designed a pair of CRISPR small guide RNAs (sgRNAs) to target the RNase III domain closest to the C terminus of *slDCL2a* and *slDCL2b* (Supplemental Fig. S2A) and transformed them into tomato as part of an integrated construct with Cas9. Of the several T0 plants with edited *slDCL2a* or *slDCL2b*, we selected two for further analysis. Both plants carried the same deletion of two codons and an isoleucine-to-valine substitution in the slDCL2a RNase domain but had different premature stop codons in slDCL2b (Supplemental Fig. S2B,C). These alleles (*sldcl2a-1*, *sldcl2b-1*, and *sldcl2b-2*) have mutations in a highly conserved region of DCL2 (Supplemental Fig. S2D), and it is likely that they would encode nonfunctional proteins.

The selfed progeny of these T0 plants in which the CRISPR/Cas9 transgene was lost by segregation are *sldcl2a-1 sldcl2b-1*, *sldcl2a-1 sldcl2b-2*, *sldcl2a-1*, *sldcl2b-1*, or *sldcl2b-2*, depending on whether they carried one or both of the mutations in the homozygous condition (Supplemental Table S1). Transcript levels of *slDCL2a* and *slDCL2b* were similar or slightly higher in *sldcl2a-1 sldcl2b-1*/*sldcl2a-1 sldcl2b-2* (referred to here as *dcl2ab*) than in M82 wild type (Supplemental Fig. S3), indicating that the mutations do not cause transcript degradation through mRNA decay. There was similarly no effect on other *DCL* mRNAs (Supplemental Fig. S3), and it is therefore unlikely that the loss of DCL2 results in compensating changes in other DCLs.

slDCL2a/slDCL2b affects endogenous 22- and 24-nt sRNA accumulation

Although DCL2 plays crucial roles in sense transgene-induced silencing and transitivity of hairpin-induced transgene silencing (Mlotshwa et al. 2008), it may also back up DCL4 in the production of sRNAs from viral and endogenous RNAs (Gasciolli et al. 2005; Bouché et al. 2006; Wu et al. 2017). Until now, however, there has been no analysis of sRNA from endogenous loci dependent on DCL2 in the presence of DCL4 that could be informative about a DCL4-independent role.

To investigate this possibility, we sequenced sRNA in wild-type and *dcl2ab* tomato leaves and found the predominant size class of sRNA was 24 nt with small amounts of 21-nt species (Fig. 1A) in both genotypes. The lack of a severe development phenotype (Supplemental Fig. S4) in *dcl2ab* indicates that the mutations did not lead to loss of essential sRNA species. Of the 642,444 sRNAs, there were 2432 (0.4%) with differential accumulation between wild type and *dcl2ab*, of which 1779

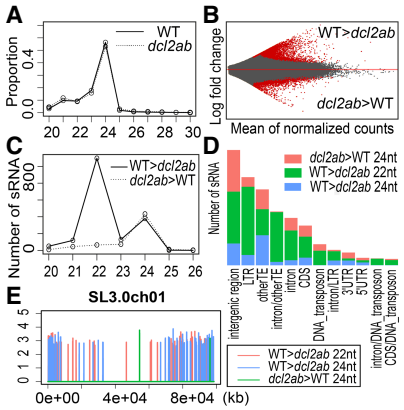

Figure 1. slDCL2a and slDCL2b are responsible for endogenous sRNA biogenesis. High-throughput sequencing data of sRNAs in 24-d-old leaves of wild type and *dcl2ab* mapped to tomato genome SL3.0. (*A*) sRNA size profile in wild type and *dcl2ab*, respectively. (*B*) MA plot showing differential analysis of sRNAs between wild type and *dcl2ab*. sRNAs that are differentially expressed (DE) (adjusted *P*-value < 0.01, calculated by DESeq2) are in red. (*C*) Length distribution of DE sRNA. (*D*) Genomic feature analysis of 22-nt D2 sRNA and 24-nt DE sRNA. The *Y*-axis shows the number of DE sRNA in each category of genomic feature. (*E*) Chromosomal distributions of 22-nt D2 loci and 24-nt DE loci. The *X*-axis shows the chromosomal coordinates, and the *Y*-axis shows the $\log_{10}$ values of sRNA reads number in wild type and *dcl2ab* for D2 and D2i loci, respectively.

were less abundant in *dcl2ab* (slDCL2-dependent sRNA-D2 sRNA) and 653 were more abundant (slDCL2-inhibited sRNA-D2i sRNA) (Fig. 1B; Supplemental Tables S2, S3). The D2 sRNAs were predominantly 22 nt (Fig. 1C), consistent with the role of DCL2 in 22-nt sRNA biogenesis, as is likely in *Arabidopsis* (Gasciolli et al. 2005; Bouché et al. 2006). In addition, there was a minor 24-nt peak (Fig. 1C) in both D2 and D2i sRNA that implies positive and negative roles of DCL2 in 24-nt sRNA pathways.

The 22-nt D2 sRNAs were predominantly from transposable elements (TEs) (Fig. 1D), indicating that slDCL2a/slDCL2b plays a role in genome stability. In contrast, the D2 and D2i 24-nt sRNAs were mostly from intergenic regions (Fig. 1D). There was also a difference in the chromosomal distribution of these differentially expressed (DE) sRNA.

The genomic loci producing 22-nt D2 sRNA revealed by SegmentSeq (Hardcastle et al. 2012) were distributed evenly across chromosomes, whereas those with 24-nt DE sRNAs were in the distal regions (Fig. 1E; Supplemental Fig. S5) that, in the tomato genome, correspond to euchromatin (Tomato Genome Consortium 2012).

Our interpretation of these findings is that slDCL2a/slDCL2b produces 22-nt D2 sRNA directly by cleavage of precursor RNAs. The 24-nt D2 sRNAs are likely to be secondary sRNAs that may be dependent on a 22-nt D2 sRNA, as in monocots (Johnson et al. 2009). According to this idea, the D2 loci with predominantly 22-nt sRNAs (Supplemental Fig. S6) would be largely made up of primary sRNAs generated by DCL2. The D2 loci with predominantly 24-nt sRNA (Supplemental Fig. S6) would be largely secondary sRNA loci. Consistent with the role of DCL2 in the release of 22-nt D2 sRNAs, the precursors of four D2 sRNA loci accumulated at higher levels in *dcl2ab* than in wild type (Supplemental Fig. S7).

The D2i sRNAs of all size classes are likely to be derived from precursor RNAs that are normally processed by slDCL2 but, in the *dcl2ab* plants, are available for other DCL proteins (Nagano et al. 2014). Consistent with this proposal, the 24-nt D2i sRNA regions produced sRNA that was predominantly 22 nt in wild-type plants (Supplemental Fig. S8). The precursors of two D2i loci were similarly abundant in wild type and *dcl2ab* (Supplemental Fig. S7), consistent with processing by DCL2 in wild type into 22-nt sRNA and a substitute DCL producing 24-nt sRNA in *dcl2ab*.

slDCL2a/slDCL2b-dependent 22-nt miRNAs

To find out whether the D2 22-nt sRNAs included miRNAs, we compared the abundance of tomato miRNA reads in the sRNA sequencing (sRNA-seq) data sets of wild type and *dcl2ab*. All of the 21-nt miRNAs and most of 22-nt miRNAs did not show statistically significant differences ($P < 0.01$) (Fig. 2A). The main exception, however, was the 22-nt miRNA: miR6026 (Fig. 2A,B). Consistent with the sRNA-seq data, the level of miR6026 detected by Northern blotting of RNA from 24-d-old leaves was lower than wild type in *dcl2b* and much lower in *dcl2ab* (Fig. 2C). By comparison, the 22-nt miR482e was at the same level in wild-type and mutant genotypes (Fig. 2C). In contrast, most miRNAs, including miR482e, were down-regulated in the slDCL1 knockdown line (Kravchik et al. 2014) compared with control, whereas miR6026 was not affected by slDCL1 knockdown (Supplemental Fig. S9). Therefore, we conclude that miR6026 is unusual among miRNAs in that it is slDCL2-dependent.

The most straightforward interpretation of these data is that the *MIR6026* precursor is cleaved by DCL2 to release miR6026. Other possibilities are that other DCL proteins carry out the cleavage and that DCL2 merely stabilizes the processed miR6026 or its precursor. The former possibility is unlikely because DCL2 has no role in stabilizing other 22-nt miRNAs, and the latter can be ruled out because there are 21-nt sRNAs from the stem–loop in the *MIR6026* precursor RNA that are unaffected by *dcl2ab* (Supplemental Fig. S10). An effect on the precursor is also ruled out because there are similar levels of pre-miR6026 in wild type and *dcl2ab* (Supplemental Fig. S7).

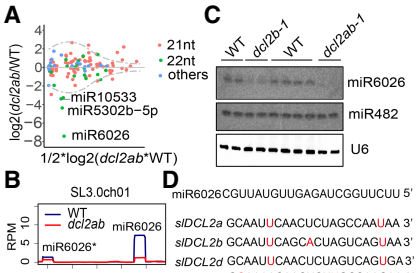

Figure 2. slDCL2a and slDCL2b are required for biogenesis of miR6026. (*A*) MA plot showing miRNA abundance in wild type and *dcl2ab*. Different sizes of miRNAs are shown in different colors. miR6026, miR5302b-5p, and miR10533 are marked. (*B*) sRNA RPM plots showing reduced accumulations of miR6026 in *dcl2ab* as compared with wild type. Mature miR6026 and miR6026* are marked. (*C*) Northern blots of miR6026 and miR482e with total RNA extracted from 24-d-old leaves of wild type and *dcl2b* and *dcl2ab* mutants, with U6 as a loading control. (*D*) Sequences of miR6026 and potential targets. Mismatches are shown in red.

The 22-nt miRNAs in *Arabidopsis* trigger secondary sRNA production using their RNA targets as a template (Chen et al. 2010; Cuperus et al. 2010), and, correspondingly, in tomato, there were sRNAs corresponding to the miR6026 potential target mRNAs (Fig. 2D; Supplemental Table S4) that include the mRNAs for *slDCL2a*, *slDCL2b*, *slDCL2d*, and a disease resistance gene: *slTM2* (Fig. 3; Supplemental Fig. S11; Li et al. 2011; Kravchik et al. 2014; Wu et al. 2016). These sRNAs were predominantly 21 nt in length and aligned with the 3′ side of the miRNA target site (Fig. 3; Supplemental Fig. S11). The sRNAs from *slDCL2a/b/d*, like many secondary sRNAs, were predominantly in a phased register corresponding to the miRNA-directed cleavage site. This phasing pattern was most pronounced in the regions adjacent to the miRNA target (Fig. 3; Supplemental Fig. S11). The phasing of the *slDCL2* sRNAs is less pronounced than with the *trans*-acting siRNA (tasiRNA) loci in *Arabidopsis.* To explain this difference, we propose that the 22-nt secondary sRNAs (Supplemental Table S5) from the *slDCL2* mRNAs could act in *cis* and trigger additional rounds of secondary sRNA in various phasing registers.

The sRNAs of *slDCL2a*, *slDCL2b*, and *slDCL2d* are dependent on slRDR6 and partially on slDCL4 (Supplemental Fig. S12), and therefore their biogenesis is like that of the well-known phased siRNA (phasiRNA)/tasiRNA and epigenetically activated siRNA (easiRNA) biogenesis in *Arabidopsis* (Allen et al. 2005; Zhai et al. 2011; Creasey et al. 2014). A crucial difference, however, is that the miR6026 is DCL2-dependent, and therefore there is a feedback component to the system. The triggers of *Arabidopsis* phasi/tasiRNA and easiRNAs are 22 nt, similar to miR6026, but are dependent on DCL1 rather than DCL2 (Cuperus et al. 2010).

Our characterization of miR6026 provides the first example of non-DCL1 processed miRNA in plants with a validated target RNA (Supplemental Fig. S9). There are other 22-nt miRNAs, but they are dependent on DCL1 (Cuperus et al. 2010), and their size is determined by an asymmetric bulge in the miRNA/miRNA* (Supplemental Fig. S13). The 22-nt miR6026 has a precursor that is symmetrical in the miRNA/miRNA* region, and its size is likely to be influenced by the DCL2 protein, as for the 22-nt D2 sRNAs, rather than by the structure of the miRNA precursor.

Of the tomato 22-nt miRNAs, there are three others (in addition to miR6026) that have symmetric structures in the miRNA/miRNA* duplex: miR5302b-5p, miR10533, and miR828. The former two are reduced in the *dcl2ab* samples (Fig. 2A) but not as much as miR6026. We predicted potential target genes of miR5302b-5p and miR10533 (Supplemental Table S6); however, none of them produced sRNA in wild type according to the sRNA-seq data (data not shown). The miR828 is expressed only at low abundance so that differential expression in the *dcl2ab* mutant cannot be assessed (data not shown), but the phased secondary sRNAs from its *TAS4* target locus (Singh et al. 2016) were less abundant in the *dcl2ab* mutant (Supplemental Fig. S14). It is therefore likely that both of these other 22-nt miRNAs with symmetrical precursors are DCL2-dependent, like miR6026, although it is not clear whether miR5302 or miR10533 triggers secondary siRNA.

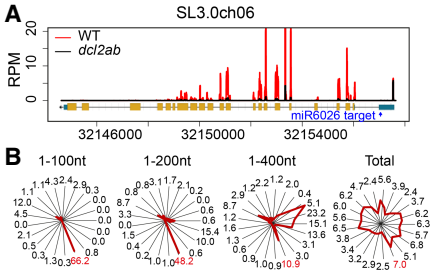

Figure 3. Accumulation of *slDCL2a* sRNAs is reduced in *dcl2ab*. (*A*) sRNA RPM plots showing the levels of slDCL2b sRNAs in wild type and *dcl2ab*. (Rectangles) Exons; (lines) genes; (cyan) untranslated regions (UTRs); (yellow) ORFs. An arrow marks the direction of transcription. The target site of miR6026 is marked with a blue arrow. (*B*) The phasing of *slDCL2a* sRNAs in wild type. Radar plots show the percentages of 21-nt reads corresponding to each of the 21 registers from the whole transcript of *slDCL2a* or 1–100 nt, 1–200 nt, or 1–400 nt of the *slDCL2a* transcript (the distance from the miR6026 cleavage position) in wild-type sRNA-seq data. The percentage of register of the 10th position and the miR6026-guided cleavage site between the 10th and 11th nucleotide of miR6026 are marked in red.

The biological function of slDCL2-dependent miR6026

To explore the biological function of miR6026, we transgenically expressed a noncoding RNA with two tandem repeats of a miR6026 target mimic site. Like the endogenous target mimic RNAs of miR399 (Puga et al. 2007), these RNAs were designed to have a 3-nt bulge at positions 10 and 11 of the miRNA-binding site (Fig. 4A). We predicted that this RNA would lock the miR6026 into a nonproductive interaction that would compete with the normal binding to *slDCL2a*, *slDCL2b*, *slDCL2d*, and *slTM2* mRNAs.

Transgenic tomato lines with high (L2 and L6) or low (L7) expression levels of the target mimic RNA grew normally under growth chamber conditions (Fig. 4B,C) and set fruit and seed as well as wild-type plants. There was a negative correlation between miR6026 accumulation and the target mimic RNA in these plants (Fig. 4B), indicating that the target mimic RNA reduces the cognate miRNA abundance, as in other examples (Yan et al. 2012). This target mimic RNA effect was highly specific so that the only affected miRNA in the L6 lines was miR6026 (*P*-value cutoff, $P < 0.05$) (Supplemental Fig. S15). Correspondingly, there was up-regulation of *slDCL2a* and, to a lesser extent, *slDCL2b* that correlated with the levels of the target mimic RNA (Fig. 4D).

An sRNA-seq analysis of two independent T1 plants from L6 and L7 confirmed that the level of miR6026 was lower in L6 than L7 (Supplemental Fig. S15) and that there was a parallel effect on secondary sRNA from *slDCL2a*, *slDCL2b*, and *slDCL2d* (Fig. 4E). In contrast, the *slTM2* sRNA and mRNA were not affected (Fig. 4E; Supplemental Fig. S16). To further validate miR6026-directed target cleavage, we assayed for miR6026 cleavage sites of *slDCL2a*, *slDCL2b*, and *slDCL2d* mRNAs with 5′-RLM-RACE (RNA ligase-mediated rapid amplification of cDNA ends). In each instance, the predicted cleaved products for miR6026 were amplified in wild-type rather than *dcl2ab* or target mimic lines (Supplemental Fig. S16).

These findings confirm that miR6026 targets mRNAs of *slDCL2a*, *slDCL2b*, and *slDCL2d* in vivo and that it is responsible for the *slDCL2* secondary sRNA production. These findings also explain the higher mRNA levels of *slDCL2a* and *slDCL2b* in *dcl2ab* than in wild type (Supplemental Fig. S3B). The lack of an effect on *slTM2* sRNA is likely because other miRNAs target the *slTM2* mRNA and could trigger secondary siRNA in the absence of miR6026 (Supplemental Figs. S11F, S17; Li et al. 2011).

The increased abundance of *slDCL2a* and *slDCL2b* RNA in L6 (strong mimic line) relative to wild-type lines (Fig. 4D) should influence the levels of endogenous D2 and D2i sRNAs (Fig. 1) and exogenous viral sRNAs (Xie et al. 2004; Bouché et al. 2006). Consistent with these predictions, there was a trend for the endogenous D2 sRNAs to increase more in L6 than in L7 and for the D2i sRNAs to be less abundant (Supplemental Fig. S18). The effect on D2 sRNAs was clearest with the 22-nt species and the 24-nt D2i sRNAs (Supplemental Fig. S18).

The potential involvement of DCL2 in viral sRNA production was supported by the increase in *slDCL2b* mRNA in TMV- and PVX-infected tomatoes (Fig. 5A) and the enhanced viral symptoms in *dcl2ab* relative to wild type (Fig. 5B,C). The TMV-infected mutant plants had "wiry" (Lesley 1928) or shoestring-like leaves, whereas infected wild-type plants had chlorosis without leaf distortion (Fig. 5B; Supplemental Fig. S19). PVX-infected *dcl2ab* plants were dead 2 wk after inoculation, in contrast to the wild-type plants that survived, although with growth stunting and leaf distortion (Fig. 5C). Consistent with the up-regulation of *slDCL2b* upon virus infection (Fig. 5A), the TMV-infected *dcl2b* had "wiry" leaves, as with infected *dcl2ab* (Supplemental Fig. S20). However, at 34 d after infection, the TMV symptoms were milder on *dcl2b* than on *dcl2ab* (Supplemental Fig. S20), consistent with a role of slDCL2a in the late stages of antiviral defense.

The antiviral activity of DCL2 was confirmed by the sRNA profiles of TMV-infected wild type and *dcl2ab*. In *dcl2ab*, the 22-nt viral sRNAs were less abundant than in wild type (Supplemental Fig. S21), whereas 21-nt viral sRNAs were increased (Supplemental Fig. S21), possibly due to compensating activity of DCL4.

Also consistent with an antiviral role of DCL2, the 22-nt sRNAs in TMV-infected L6 were more abundant than in wild-type plants (Supplemental Fig. S21). In addition,

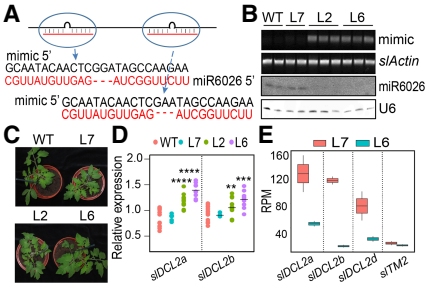

Figure 4. miR6026 targets *slDCL2a/b/d* transcripts and triggers secondary sRNA production. (*A*) Diagram of miR6026 target mimic. (*B*, *top* to *bottom*) Semiquantitative RT–PCR of miR6026 mimic RNA in wild-type and different mimicry lines with *slActin7* as control. Northern blots of miR6026 with U6 as a loading control. (*C*) Three-week-old plants of wild type and one weak mimic line (L7) and two strong mimic lines of miR6026 (L2 and L6). (*D*) Quantitative RT–PCR (qRT–PCR) of *slDCL2a* and *slDCL2b* in wild-type and mimicry lines. (**) $P < 0.01$; (***) $P < 0.001$; (****) $P < 0.0001$. (*E*) RPM plot of total reads mapped to potential target transcripts of miR6026 in a weak mimic line (L7) and a strong mimic line (L6).

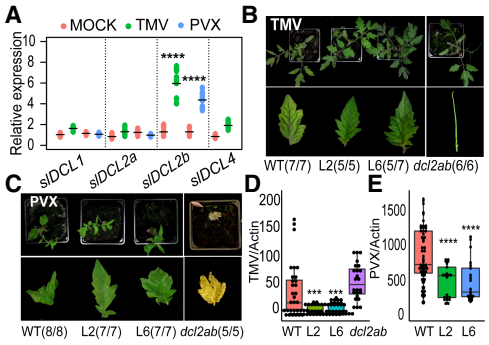

Figure 5. slDCL2a and slDCL2b are required for tomato antivirus defense against TMV and PVX. (*A*) qRT–PCR results of slDCLs in mock- and virus-infected samples. *slActin7* was used as an endogenous control. (*B*) Two weeks after TMV inoculation, the plants showed chlorosis (wild type [WT]), weak chlorosis (L2 and L6), and "shoestring" (*dcl2ab*) symptoms of TMV. Numbers in parenthesis show the number of plants with the indicated symptoms and the number of infected plants. (*C*) Two weeks after PVX inoculation, the plants showed growth stunting and leaf distortion symptoms (wild type [WT] and target mimic lines L2 and L6) or lethality (*dcl2ab*). Numbers in parenthesis show the number of plants with the indicated symptoms and the number of infected plants. (*D*,*E*) Real-time PCR analysis of TMV and PVX in infected plants. *slActin7* was used as a control. (***) $P < 0.001$; (****) $P < 0.0001$.

there were fainter chlorotic symptoms than in wild type (Fig. 5B; Supplemental Fig. S19), and viral RNA accumulation was reduced (Fig. 5D). There was also less viral RNA accumulation in PVX-infected mimic plants than in wild type (Fig. 5E), although the viral symptoms were similar (Fig. 5C).

The reduction of symptoms or virus infection in the TMV-infected plants is likely due to DCL2/miR6026 because the TMV symptoms in the progeny of L6 × *dcl2b* or *dcl2ab* were as severe as in *dcl2b* and *dcl2ab* (Supplemental Fig. S22). From these results, we conclude that the DCL2-miR6026 feedback influences the effect of RNA silencing on viral RNA accumulation and viral disease progression in tomato (Supplemental Fig. S23).

This analysis of slDCL2 has both applied and basic science implications. At the applied level, we demonstrated that disease resistance can be enhanced by blocking a miRNA that targets a defense mRNA (Fig. 5). In our L6 lines, this effect was achieved without inhibition of basic features in growth and development (Fig. 4C), although a more detailed phenotypic analysis remains to be carried out. The potential of this approach is also confirmed by findings of enhanced resistance to soybean mosaic virus (SMV) (Bao et al. 2018) and *Phytophthora infestans* (Jiang et al. 2018) in other lines in which defense mRNAs were elevated by miRNA target site mimics. There are multiple miRNAs, including miR403 (Harvey et al. 2011) and the miR482 family (Shivaprasad et al. 2012), that, like miR6026, target defense proteins. Although the effect of any single defense miRNA mimic may be weak (Fig. 5), it could be that strong resistance can be achieved by combining several of these RNAs in a single line.

The fundamental science advance of this work is through the finding that there are endogenous 22-nt sRNA products of DCL2, including the miRNAs (Figs. 1, 2). The finding of DCL2-dependent siRNAs had been suspected previously from the analysis of *DCL2* in *Arabidopsis* (Xie et al. 2004; Bouché et al. 2006) but not shown directly unless the plants also lacked DCL4. We also show that there are D2 sRNAs and D2i sRNAs that are predominantly 24 nt in length (Fig. 1C–E). The DCL2 effect on 24-nt sRNAs is most likely indirect and could influence the epigenome of tomato through the RNA–direct DNA methylation pathway (Nuthikattu et al. 2013). From these various findings, it is clear that DCL2 is not merely a backup for DCL4 but an important component of the diverse RNA silencing pathways of plants.

Materials and methods

Plant materials

All tomato plants used in this study were *Solanum lycopersicum* cv M82. CRISPR/Cas9 mutants were obtained by stably transforming tomato plants as described previously (Gouil and Baulcombe 2016). For target mimicry plants, two tandem repeats of miR6026 target mimic were cloned into the gateway construct pGWB402Ω and then transformed into tomato. Primers for cloning and genotyping are listed in Supplemental Table S7.

For virus infection, 3-wk-old plants of *Nicotiana benthamiana* were rub-inoculated with TMV U1 virion or infiltrated with agrobacteria carrying pGR106 for PVX (Harris et al. 2013). After 1 wk, *N. benthamiana* leaves were harvested and ground to sap, which was rubbed onto 10-d-old tomato cotyledons for inoculation.

RNA analyses

Total RNA was extracted by the TRIzol method. Northern blotting and sRNA library preparation were performed as described (Shivaprasad et al. 2012). RT–PCR was performed as described (Harris et al. 2013). 5′-RLM-RACE was performed following the instruction of the GeneRacer kit (Life Technologies). Primers are listed in Supplemental Table S7.

Bioinformatics

The sRNA reads were trimmed using Trimgalore and mapped to the Heinz genome SL3.0 or respective genes using Bowtie (Langmead et al. 2009) with specified parameters of -m 1 and -v 0. The bam files were used for differential sRNA analysis by SegmentSeq (Hardcastle et al. 2012) and DESeq2 (Love et al. 2014) after filtering out those sRNAs with less than five sequencing reads in five libraries. The raw sequencing data are available in the NCBI Sequence Read Archive database under accession number SRP127908.

Phasing analysis of sRNA was performed by counting 21-nt sRNA mapped to each of 21 registers in each gene. Register 1–21 represents the distance of the sRNA starting site from 5′ of miR6026. Percentages of 21-nt reads corresponding to each of the 21 registers from each gene are shown by radar plots.

Analyses of miRNA were performed based on a tomato miRNA list (Supplemental Table S8) combining 92 miRNAs from miRBase22 and 30 miRNAs from recent publications.

Acknowledgments

We are grateful to Dr. John Carr for providing virus material and help. We thank Mel Steer and James Barlow for technical assistance. We thank Dr. Betty Chung, Dr. Sara Lopez-Gomollon, Dr. Claudia dos santos Martinho, Dr. Francisco Navarro, and Dr. Adrian Valli for helpful comments and discussions. We also thank Dr. Ming-Tsung Wu for assistance with RLM-RACE analysis. This work was supported by European Research Council Advanced Investigator grant ERC-2013-AdG 340642 (Transgressive Inheritance in plant Breeding and Evolution [TRIBE]), the Royal Society (RP170001), and the Balzan Foundation. D.C.B. is the Royal Society Edward Penley Abraham Research Professor.

Author contributions: Experiments were designed by Z.W. and D.C.B. and performed by Z.W., A.C.P., W.H.Y., and S.T. Bioinformatics analysis was performed by Z.W. and T.J.H. The manuscript was prepared by Z.W. and D.C.B.

References

Allen E, Xie Z, Gustafson AM, Carrington JC. 2005. microRNA-directed phasing during *trans*-acting siRNA biogenesis in plants. *Cell* **121:** 207–221.

Bai M, Yang G-S, Chen W-T, Mao Z-C, Kang H-X, Chen G-H, Yang Y-H, Xie B-Y. 2012. Genome-wide identification of Dicer-like, Argonaute and RNA-dependent RNA polymerase gene families and their expression analyses in response to viral infection and abiotic stresses in *Solanum lycopersicum*. *Gene* **501:** 52–62.

Bao D, Ganbaatar O, Cui X, Yu R, Bao W, Falk BW, Wuriyanghan H. 2018. Down-regulation of genes coding for core RNAi components and disease resistance proteins via corresponding microRNAs might be correlated with successful soybean mosaic virus infection in soybean. *Mol Plant Pathol* **19:** 948–960.

Baulcombe D. 2004. RNA silencing in plants. *Nature* **431:** 356–363.

Bouché N, Lauressergues D, Gasciolli V, Vaucheret H. 2006. An antagonistic function for *Arabidopsis* DCL2 in development and a new function for DCL4 in generating viral siRNAs. *EMBO J* **25:** 3347–3356.

Chen H, Chen L, Patel K, Li Y, Baulcombe DC, Wu S. 2010. 22-nucleotide RNAs trigger secondary siRNA biogenesis in plants. *Proc Natl Acad Sci* **107:** 15269–15274.

Creasey KM, Zhai J, Borges F, Van Ex F, Regulski M, Meyers BC, Martienssen RA. 2014. miRNAs trigger widespread epigenetically activated siRNAs from transposons in *Arabidopsis*. *Nature* **508:** 411–415.

Cuperus JT, Carbonell A, Fahlgren N, Garcia-ruiz H, Burke RT, Takeda A, Sullivan CM, Gilbert SD, Montgomery TA, Carrington JC. 2010. Unique functionality of 22-nt miRNAs in triggering RDR6-dependent siRNA biogenesis from target transcripts in *Arabidopsis*. *Nat Struct Mol Biol* **17:** 997–1004.

Gasciolli V, Mallory AC, Bartel DP, Vaucheret H. 2005. Partially redundant functions of *Arabidopsis* DICER-like enzymes and a role for DCL4 in producing *trans*-acting siRNAs. *Curr Biol* **15:** 1494–1500.

Gouil Q, Baulcombe DC. 2016. DNA methylation signatures of the plant chromomethyltransferases. *PLOS Genet* **12:** e1006526.

Hardcastle TJ, Kelly KA, Baulcombe DC. 2012. Identifying small interfering RNA loci from high-throughput sequencing data. *Bioinformatics* **28:** 457–463.

Harris CJ, Slootweg EJ, Goverse A, Baulcombe DC. 2013. Stepwise artificial evolution of a plant disease resistance gene. *Proc Natl Acad Sci* **110:** 21189–21194.

Harvey JJW, Lewsey MG, Patel K, Westwood J, Heimsta S, Baulcombe DC. 2011. An antiviral defense role of AGO2 in plants. *PLoS One* **6:** e14639.

Jiang N, Meng J, Cui J, Sun G, Luan Y. 2018. Function identification of miR482b, a negative regulator during tomato resistance to *Phytophthora infestans*. *Hortic Res* **5:** 9.

Johnson C, Kasprzewska A, Tennessen K, Fernandes J, Nan G, Walbot V, Sundaresan V, Vance V, Bowman LH. 2009. Clusters and superclusters of phased small RNAs in the developing inflorescence of rice. *Genome Res* **19:** 1429–1440.

Kravchik M, Sunkar R, Damodharan S, Stav R, Zohar M, Isaacson T. 2014. Global and local perturbation of the tomato microRNA pathway by a trans-activated *DICER-LIKE 1* mutant. *J Exp Bot* **65:** 725–739.

Langmead B, Trapnell C, Pop M, Salzberg SL. 2009. Ultrafast and memory-efficient alignment of short DNA sequences to the human genome. *Genome Biol* **10:** R25.

Law JA, Jacobsen SE. 2011. Establishing, maintaining and modifying DNA methylation patterns in plants and animals. *Nat Rev Genet* **11:** 204–220.

Lesley MM. 1928. The 'wiry' tomato: a recessive mutant form resembling a plant affected with mosaic disease. *J Hered* **8:** 337–344.

Li F, Pignatta D, Bendix C, Brunkard JO, Cohn MM, Tung J, Sun H. 2011. MicroRNA regulation of plant innate immune receptors. *Proc Natl Acad Sci* **109:** 1790–1795.

Love MI, Huber W, Anders S. 2014. Moderated estimation of fold change and dispersion for RNA-seq data with DESeq2. *Genome Biol* **15:** 1–21.

Mlotshwa S, Pruss GJ, Peragine A, Endres MW, Li J, Chen X, Poethig RS, Bowman LH, Vance V. 2008. *Dicer-like2* plays a primary role in transitive silencing of transgenes in *Arabidopsis*. *PLoS One* **3:** e1755.

Nagano H, Fukudome A, Hiraguri A, Moriyama H, Fukuhara T. 2014. Distinct substrate specificities of *Arabidopsis* DCL3 and DCL4. *Nucleic Acids Res* **42:** 1845–1856.

Nuthikattu S, Mccue AD, Panda K, Fultz D, Defraia C, Thomas EN, Slotkin RK. 2013. The initiation of epigenetic silencing of active transposable elements is triggered by RDR6. *Plant Physiol* **162:** 116–131.

Parent JS, Bouteiller N, Elmayan T, Vaucheret H. 2015. Respective contributions of *Arabidopsis* DCL2 and DCL4 to RNA silencing. *Plant J* **81:** 223–232.

Puga I, Franco-zorrilla M, Todesco M, Mateos I, Paz-ares J, Rubio-somoza I, Leyva A, Weigel D, Garcı JA. 2007. Target mimicry provides a new mechanism for regulation of microRNA activity. *Nat Genet* **39:** 1033–1037.

Rogers K, Chen X. 2013. Biogenesis, turnover, and mode of action of plant microRNAs. *Plant Cell* **25:** 2383–2399.

Shivaprasad PV, Chen H-M, Patel K, Bond DM, Santos BACM, Baulcombe DC. 2012. A microRNA superfamily regulates nucleotide binding site-leucine-rich repeats and other mRNAs. *Plant Cell* **24:** 859–874.

Singh A, Saraf S, Dasgupta I, Mukherjee SK. 2016. Identification and validation of a virus-inducible ta-siRNA-generating TAS4 locus in tomato. *J Biosci* **41:** 109–118.

Taochy C, Gursanscky NR, Cao J, Fletcher SJ, Dressel U, Mitter N, Tucker MR, Koltunow AM, Bowman JL, Vaucheret H, et al. 2017. A genetic screen for impaired systemic RNAi highlights the crucial role of Dicer-like 2. *Plant Physiol* **176:** 01181.2017.

Tomato Genome Consortium G. 2012. The tomato genome sequence provides insights into fleshy fruit evolution. *Nature* **485:** 635–641.

Wu P, Wu Y, Liu C-C, Liu L-W, Ma F-F, Wu X-Y, Wu M, Hang Y-Y, Chen J-Q, Shao Z-Q, et al. 2016. Identification of *Arbuscular mycorrhiza* (AM)-responsive microRNAs in tomato. *Front Plant Sci* **7:** 429.

Wu YY, Hou BH, Lee WC, Lu SH, Yang CJ, Vaucheret H, Chen HM. 2017. DCL2- and RDR6-dependent transitive silencing of *SMXL4* and *SMXL5* in *Arabidopsis dcl4* mutants causes defective phloem transport and carbohydrate over-accumulation. *Plant J* **90:** 1064–1078.

Xie Z, Johansen LK, Gustafson AM, Kasschau KD, Lellis AD, Zilberman D, Jacobsen SE, Carrington JC. 2004. Genetic and functional diversification of small RNA pathways in plants. *PLoS Biol* **2:** 642–652.

Yan J, Gu Y, Jia X, Kang W, Pan S, Tang X, Chen X, Tang G. 2012. Effective small RNA destruction by the expression of a short tandem target mimic in *Arabidopsis*. *Plant Cell* **24:** 1–14.

Zhai J, Jeong D, De Paoli E, Park S, Rosen BD, Yan Z, Kitto SL, Grusak MA, Jackson SA, Li Y, et al. 2011. MicroRNAs as master regulators of the plant *NB-LRR* defense gene family via the production of phased, *trans*-acting siRNAs. *Genes Dev* **25:** 2540–2553.